Proceedings of the Eighth Meeting of the International Collaboration on Advanced Neutron Sources (ICANS-VIII)
8-12 July 1985, Rutherford Appleton Laboratory Report RAL-85-110

Status of the Intense Pulsed Neutron Source*

John M. Carpenter, Bruce S. Brown,
Robert L. Kustom, Gerard H. Lander,
Charles W. Potts, August W. Schulke
Argonne National Laboratory
Argonne, Illinois 60439 USA

and

Gödehard Wüstefeld
Argonne National Laboratory and KFA Jülich

Introduction

Fortunately in spite of some premature reports of its impending demise, IPNS has passed the fourth anniversary of the first delivery of protons to the targets (May 5, 1981) and is approaching the fourth anniversary of its operation as a scattering facility (August 4, 1981). On June 10, 1984, the RCS delivered its one billionth pulse to the IPNS target--the total number of protons delivered to the targets amounted then to 75 stp cm^3 of H_2 gas! Since startup IPNS has improved steadily in terms of the performance of the Rapid Cycling Synchrotron, the source and its moderators and the scattering instruments, and a substantial and productive user program has evolved.

This report summarizes the current status of the Intense Pulsed Neutron Source at Argonne National Laboratory. We include reference to recent accelerator operating experience, neutron facility operating experience, improvements to these systems, design work on the ASPUN high-current facility, booster target design, the new solid methane moderator, characterization of the room temperature moderators, and provide some examples of recent results from several of the spectrometers.

Status of the Rapid Cycling Synchrotron

Recently RCS has run with high reliability and delivered time-average currents of 12 μA (see Figures 1 and 2). Our standard operating mode is to accelerate to 450 MeV, since the increased reliability at that energy compensates for the higher neutron yield at the design energy of 500 MeV. In the October 1984 running period RCS suffered a leak in the cooling line of the extraction septum magnet, which cost several months of availability which have been made up in the succeeding months. Recent developments have improved the performance of the accelerator, namely the installation of a new clock which enables the accelerator to run almost synchronously with the power line while still allowing the choppers to operate with high reliability, and the use of carbon stripping foils which require less conditioning than the polymer foils used until now, and seem to live longer. These improvements have led to average currents near 13 μA. At the time of shutdown for the summer on 3 July, 1985, the current was 14 μA! Other contributions [1,2] in this Meeting describe these developments in greater detail.

* Work Supported by U. S. Department of Energy

Status of the ASPUN-FFAG

Argonne is developing the design for an advanced super pulsed-spallation neutron source called ASPUN that uses a fixed-field alternating-gradient accelerator as the proton source. Work on this design has gone on at a somewhat reduced pace in the past months, due to the work on other accelerator projects of importance to the Laboratory.

The design goal for ASPUN is to deliver a peak flux greater than 1×10^{17} thermal neutrons/cm^{2}sec at the beam target with a repetition rate of somewhere between 10 Hz and 100 Hz. If a direct scaling from the IPNS target, which is currently in operation at Argonne, is reasonable, an average beam current of 1380 μA at 1500 MeV would be sufficient to achieve this neutron flux. In order to provide a sizeable safety margin in startup, the design goal for ASPUN is 3800 μA. Table 1 shows a summary of the main-ring parameters.

Table 1

ASPUN Main Ring Parameters

Injection Frequency	240 Hz
Extraction frequency	40 Hz
Injection energy (H^-)	200 MeV
Extraction energy	1500 MeV
Injection radius	25.888 m
Extraction radius	28.139 m
Number of sector magnets	20
Magnetic field (injection/extraction)	0.413 T/1.327 T
Field index k = (R/B) (dB/dR)	14
Spiral angle	61°
Horizontal acceptance	650 π mm-mrad
Vertical acceptance	500 π mm-mrad
Betatron tunes ν_x/ν_z	4.25/3.3
RF frequencies (2nd harmonic)	2.08/3.09 MHz
(1st harmonic)	1.54/1.57 MHz
Peak RF voltage per turn	400 kV
Protons per pulse (design goal) (injection/extraction)	$1 \times 10^{14}/6 \times 10^{14}$

The plans are to accelerate on the second harmonic two bunches from the injection energy to 1250 MeV. At this energy a stack of altogether 12 bunches is built up and finally accelerated as a single bunch to 1500 MeV. Extraction is accomplished in one turn with a fast kicker magnet. The pulse length of the single extracted bunch which is transported to the target is about 325 ns.

There are two possible approaches for the FFAG to get the transverse focusing (see Figures 3 and 4). Up to now, mainly the spiral focusing with normal conducting magnets was studied[3]. Recently, an investigation of radial focusing with reversed field magnets[4] showed several important advantages compared to the earlier studies. By using superconducting coils with a peak field of about 4 T, the radial FFAG can be built with the same radius as the spiral machine but with much longer effective straight sections between the magnets. Therefore, the rf cavity gap can be placed perpendicular to the beam orbit. Additionally, the stability region in the phase space will be larger and therefore the machine will be less sensitive to field and alignment errors. Nearly all the machine parameters from Table I will be unchanged. The magnetic field distribution along the azimuthal direction is given in Figure 5. The maximum positive field on the extraction orbit will be 4 T and the minimum negative field along the same orbit will be -1.3 T. The spiral angle will be zero.

Further topics which are under study and basically identical for both types of machines are beam loading and collective phenomena. First calculations show that beam loading can be controlled by a cathode follower; alternatively a feedback amplifier operating on the second harmonic could correct the waveform distortion. The transverse coherent instability is a critical issue and needs to be studied in much more detail. The outcome of this study might indicate an increase in the injection energy.

Target Station Developments

It is a pleasure to report that the target and its cooling, monitoring and other associated systems have continued to operate with no significant problems. Two of the most significant accomplishments of the past year which relate to the neutron source itself, are the installation of a new solid methane moderator, and the characterization of the pulse shapes of the room temperature polyethylene moderators.

Continuing what is now a long sequence of moderator developments at IPNS, we have installed a grooved, solid methane moderator which operatoes at a physical temperature of 12 K, and produces a spectrum with a temperature of 20 K. The system has operated quite well since its installation in January, 1985, and the increased intensity of long wavelength neutrons has brought our cold neutron instruments up to a high level of performance. Figure 6 shows the spectrum of neutrons from the new moderator. Another paper provides more details on the new system[5].

With Susumu Ikeda, who visited us from KEK, we have performed careful measurements of the pulse shapes as a function of energy for the two ambient-temperature polyethylene moderators. The result is a new set of functions which fit the pulse shapes in a simple and intuitively-appealing way. Ikeda's pulse shape function is of the form

$$i(v,t) = \alpha/2 \{ (1-R)(\alpha t)^2 \exp(-\alpha t) + 2\alpha^2\beta R/(\alpha-\beta)^3 [\exp(-\beta t)-\exp(-\alpha t)(1+(\alpha-\beta)t+1/2(\alpha-\beta)^2 t^2)]\} \; ; \; t>0 \qquad (1)$$

where $\int_0^\infty i(v,t)dt = 1$, $\alpha = v\Sigma$ in the slowing down time distribution, β is the decay constant of the fundamental eigenfunction (Maxwellian), and R is the ratio of the area of the second term (the "storage term") to the total area. The constants have simple wavelength dependence,

$$\Sigma = (S_1^2 + S_2^2\lambda^2)^{1/2}, \qquad (2)$$

S_1, S_2, and β are constants, and the ratio R can be represented

$$R = \exp(-E/E_o). \qquad (3)$$

For one 10x10x5 cm^3, heavily-irradiated, ambient temperature (~50 C), polyethylene moderator poisoned at 2.5 cm depth with 0.5 mm Cd, we found S_1 = 0.98 cm^{-1}, S_2 = 0.27 cm^{-1}, $1/\beta$ = 24.1 μsec and E_o = 190. meV. In Equation 1 the first term represents the escape of neutrons from the moderator while they are slowing down; the second term represents the escape of thermalized neutrons, whose exponentially-decaying population is fed by the slowing-down time distribution. The mean emission time derived from the distribution (1) is

$$\bar{t} = 3/2\alpha + R/\beta. \qquad (4)$$

Figure 7 shows the time dependence of the neutron pulse as a function of energy, resulting from a least-squares fit of Equation 1 to data between .00253 eV and 0.648 eV. A complete description of the work[6] will soon appear. These results already provide the basis for complete understanding of the chopper spectrometer resolution functions and energy transfer scales. We hope that they may also provide better profile functions and time scale calibrations for time-of-flight diffractometers.

Booster Target Development

In order to supply greater neutron beam intensities, we have launhced a program to produce an enriched uranium booster target for IPNS. The principles guiding the development have been to provide a modest gain while imposing no requirements for major changes in the target station, and producing no significant increase in the width of the primary source neutron pulse. This led to the choice of a nominal gain factor of 5, (k_{eff} = 0.80) in a fast, subcritical arrangement. The total power , about 90 kW compared to the present 10 kW, can be handled by the present cooling systems, and no major shielding changes will be needed. The neutron beam intensity gain due to the booster will be a factor of about 3, mostly because the spallation source does not couple perfectly to the most nearly critical mode of the booster. The delayed neutron background will increase from the present roughly 0.5% to about 3.0%, which we believe will require only modest measures to overcome. Figure 8 shows a cross sectional view of the booster target.

The booster design program has been in progress for about one year and we expect to install the new system to operate in Fall, 1986. Another paper[7] describes the booster project in greater detail.

Scattering Instruments and Experimental Facilities

We have made a number of improvements, modifications and additions to the scattering instruments and the facilities available to the users. Table 2 summarizes the most significant ones.

Table 2.

Summary of Improvements and Modifications of

IPNS Scattering Instruments and Experimental Facilities

Large-angle ($90^\circ < \phi < 140^\circ$) flight path installed in HRMECS

Dead time in the Anger camera of SCD improved from 15 μs to 3μs, and dead time measuring system improved

Remote-window sample chamber installed on SCD--sliding seals permit full rotation of the sample

Misplaced shielding wedge relocated in SEPD--produced ×2 intensity increase

Multiple Converging Aperture collimation installed in SAD, and sample-to detector distance shortened from 3 m to 1.5 m

Additional sample environment equipment provided

New VAX 11/750 computer installed

Figure 9 shows the new large-angle flight path of the High Resolution Medium Energy Chopper Spectrometer.

Figure 10 shows the collimating system of the Small Angle Diffractometer. The converging apertures are formed by a pair of converging Soller collimators, one vertical, the other horizontal, with approximately 1.- mm exit slits, tapered to converge at the location of the detector. CIDIC of UK produced these to our specifications, using slats of ^{11}B-painted aluminium. These work quite well in spite of a small halo (actually appears like a four-petaled flower) outside the penumbra due to internal reflections. This effect seems to be controllable by additional roughening of the surfaces, which we are investigating.

We pursue a continuing effort to provide a greater range of sample environments for research at IPNS. Table 3 summarizes the present complement of pressure cells, cryostats and ovens available at IPNS. Another paper [8] deals more completely with the peripheral equipment.

Table 3.

Equipment for Special Sample Environments at IPNS

Low Temperatures
(Adaptable to most instruments)

Displex Refrigerators	$T \geq 10$ K
^{4}He Cryostat	$1.5 \leq T \leq 200$ K

High Temperatures

Diffractometer and Chopper Spectrometer Furnaces	$T \leq 1400$ C
Small-Angle Diffractometer Furnace	$T \leq 1000$ C

High Pressures
(Special Environment Powder Diffractometer, $2\theta = 90°$)

	Pressure	Volume	Temperature
Piston-Cylinder	35 Kbar	0.25 cm^3	300 K
Gas-Pressurized Cells	6 Kbar	2.0 cm^3	10 K
Clamped Piston-Cylinder	25 Kbar	1.5 cm^3	10 K

Examples of Some Recent Scientific Results

To illustrate the performance of some of the IPNS scattering instruments, we provide some examples of recent experimental results. Figure 11 shows the scattering from superfluid Helium, measured at the Low Resolution Medium Energy Chopper Spectrometer, with incident energy E_o = 160 meV and a the scattering angle ϕ = 116 . The measurements were performed by P. Sokol, R. Simmons, D. Price and R. Hilleke. Plotted is the difference between data taken in the superfluid phase at 1.0 K, and in the normal phase at the same atom density, $1/\rho$ = 27. cm^3/mole. (We have found that the mean kinetic energy in the normal substance depends almost exclusively on the density.) The wave vector change at the peak of the scattering is about 13. $Å^{-1}$. The positive component is the resolution-broadened scattering from the zero-momentum Bose condensate. The fitted function is the difference of two gaussians; the result of the fit is that the integrated difference is zero, indicating that the area lost from the broad, normal component appears in the condensate peak. Figure 12 shows the condensate fraction n_o measured in this way.

Figure 13 shows a plot of the diffracted intensity distribution in the (4.93,k.1) plane of $(BEDT\text{-}TTF)_2I_3$, [bis(ethylenedithio)tetrathiafulvalene triiodide] at 20 K, measured at the Single Crystal Diffractometer; by Emge, et al.[8]. The sample mass was 2 mg, and the counting time for these data was 24 hours. Superlattice peaks with indices (hkl) $\pm$ q, where q = (0.08, 0.27,0.205) appear below 200 K.

Figure 14 illustrates the result of the measurement **in situ** of the scattering from CoO(1-x)O, slightly non-stoichiometric Cobalt Oxide, at 1100 C under a small partial pressure of CO. The data are those of John Faber and his colleagues. The main figure shows the data from scattering angle $2\Theta = 90°$, the Rietveld refinement, the location of the Bragg peaks and the residual of the fit. The inset shows the variation of the lattic parameter with defect concentration x (note the very small values of x). The high resolution of the instrument allowed determination of the changes in lattice parameter on the order of one part in 10^4. The inset also shows the variation of the isotropic thermal parameters of the Co and O atoms as a function of x, made possible by the measurements a small d spacings.

Figures 15a and 15b show the diffraction pattern of the collagen of kangaroo tail tendon reconstituted in D_2O, compiled from the 14. Å wavelength bin (15a) and from the 7. Å wavelength bin (15b) The long-wavelength data illustrate the low-Q range accessible ($Q_{min} = 0.0036$ Å^{-1}) and the resolution of the instrument. The shorter-wavelength data show the first six orders of reflection from the structure (the second order structure factor is zero). The instrument is now very effective, with good Q_{min} and good resolution, and the wide Q range which is characteristic of TOF Small Angle Scattering instruments; these result from the installation of the new converging aperture collimation and the new solid methane moderator.

User Program

The use of IPNS continues to increase, as do the number of users and total amount of instrument time requested. Figure 16 shows the total number of requested instrument days, those requested by non-Argonne scientists as principal investigator and the (smaller) number of instrument days available for each six month proposal period. Table 4 shows the distribution of requests for instrument time for the January 1984 proposal period. We are oversubscribed by a factor of 2.5 on average, and a factor of more than 3. on the chopper spectrometers.

Table 4.

	Requested				
	Non-ANL	ANL Instrument Scientist	ANL Other	Total	
Powder diffractometers (SEPD & GPPD)	179	11	38	227	86
Single crystal diffractometer	105	0	1	106	43
Small-angle diffractometer	36	41	16	93	43
Chopper spectrometers (HRMECS & LRMECS)	240	7	26	273	86
Crystal analyzer spectrometer	59	0	0	59	43
	619	59	80	758	301

Table 5.

	FY 1983	FY 1984
Weeks of operation	26	29
Number of experiments performed	110	210
Visitors to IPNS for at least one experiment:		
DOE labs - ANL	41	49
DOE labs - other	7	7
Other government labs	2	1
Universities	33	45
Industry	5	9
Foreign	18	39
	106	150

The users come from many institutions; Table 5 shows the distribution according to types of institution for the years 1983 and 1984. The table entries do not include multiple visits by one person in one year.

Conclusions

IPNS continues to improve and to serve a useful role in the community of facilities for condensed matter science.

References

1. A. Rauchas, F. Brumwell, C. Potts, V. Stipp and G. Volk, "Status of the Intense Pulsed Neutron Source Accelerator System", these proceedings.

2. G. E. Ostrowski, L. I. Donley, A. V. Rauchas, G. J. Volk, E. A. Jung, J. R. Haumann and C. A. Pelizzari, "The IPNS Chopper Control and Accelerator Interface Systems", these proceedings.

3. R. L. Kustom, T. K. Khoe and E. A. Crosbie, "A 1500 MeV Fixed-Field Alternating Gradient Synchrotron for a Pulsed Spallation Neutron Source", to be published in the proceedings of the Particle Accelerator Conference, Vancouver, Canada, 13 - 16 May, 1985.

4. P. F. Meads and G. Wüstefeld, "An FFAG Compressor and Accelerator Ring Studied for the German Spallation Neutron Source", to be published in the proceedings of the Particle Accelerator Conference, Vancouver, Canada, 13 - 16 May, 1985.

5. John M. Carpenter, August W. Schulke, Terry L. Scott, Denis G. Wozniak, Burton O. Benson and Bryan D. Leyda, "The IPNS Grooved, Solid Methane Moderator", these proceedings.

6. Susumu Ikeda and John M. Carpenter, "Wide-Energy-Range, High-Resolution Measurements of Neutron Pulse Shapes of Polyethylene Moderators", to be published in Nuclear Instruments and Methods in Physics Research (1985).

7. A. W. Schulke, Jr. for the IPNS Enriched Uranium Booster Target Design Team, "IPNS Enriched Uranium Booster Target", these proceedings.

8. D. E. Bohringer and R. K. Crawford, "Sample-related Peripheral Equipment at IPNS", these proceedings.

9. T. Emge, P. Leung, M. Beno, A. Schultz, L. Sowa and J. M. Williams, Phys Rev B 30, 6780 (1984).

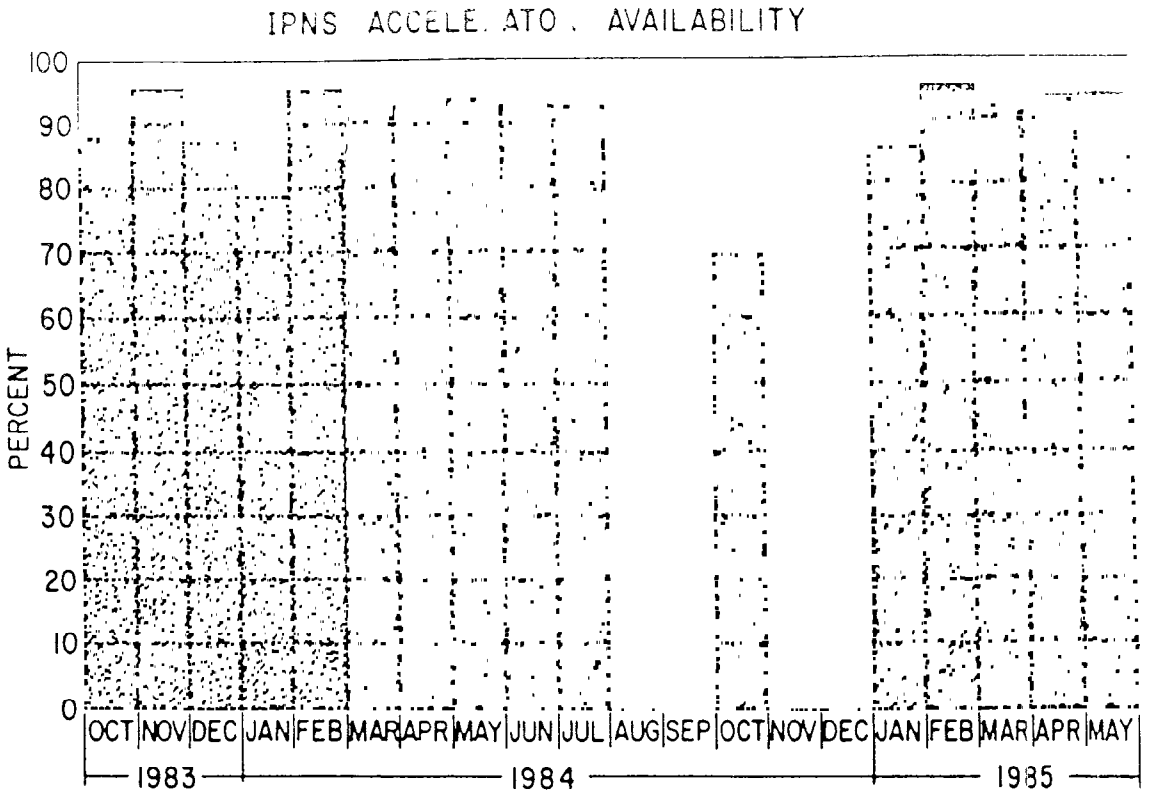

1. Availability of the Rapid Cycling Synchrotron.

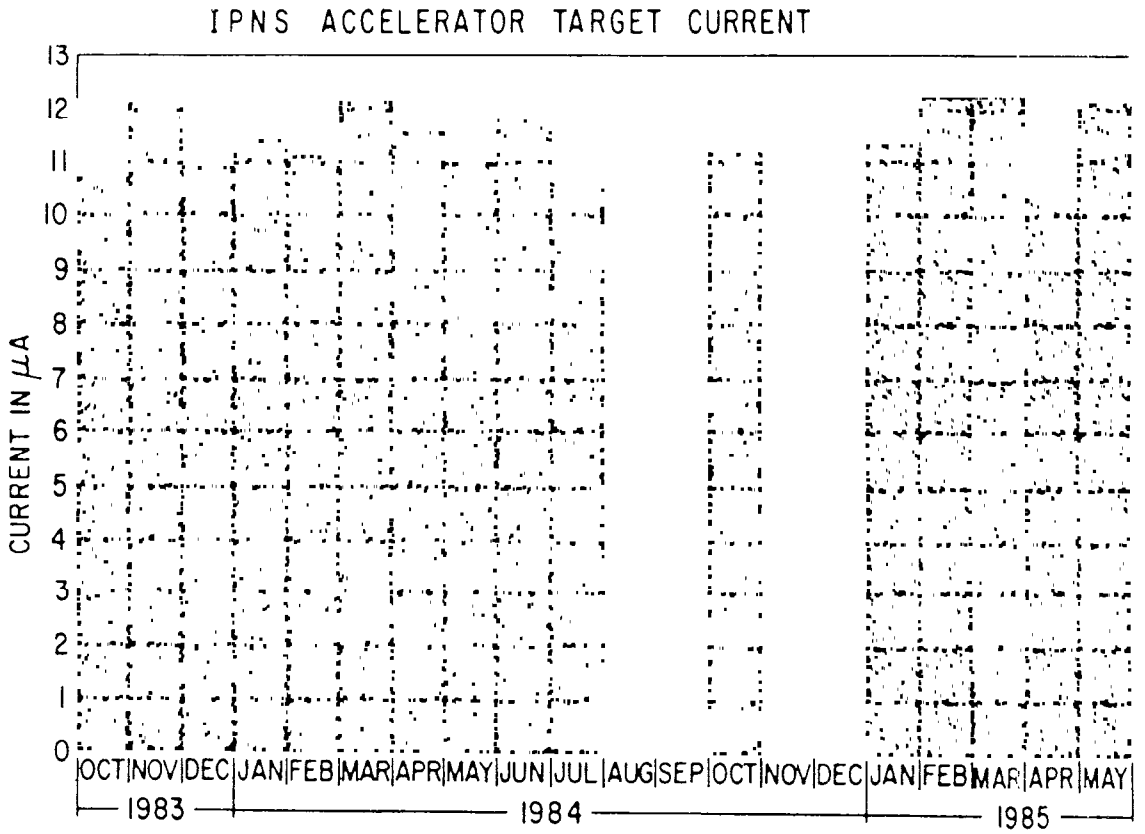

2. Average current delivered by RCS to the IPNS target (30 Hz).

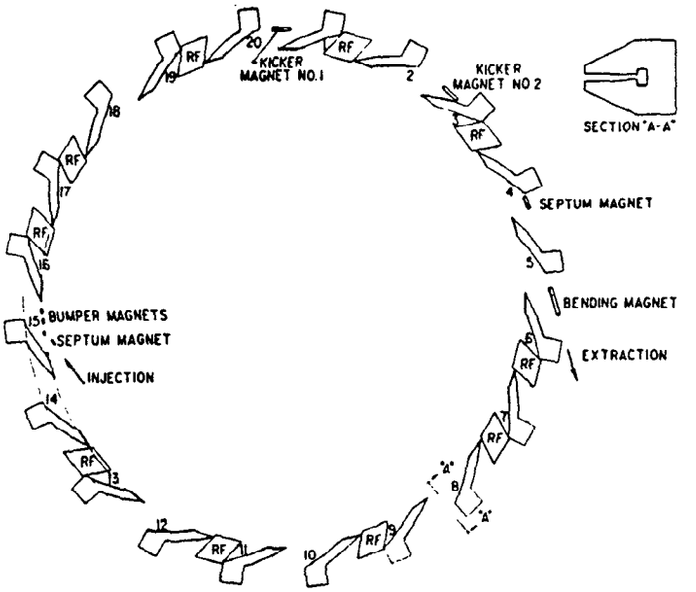

3. Schematic view of the 1500 MeV FFAG, spiral type.

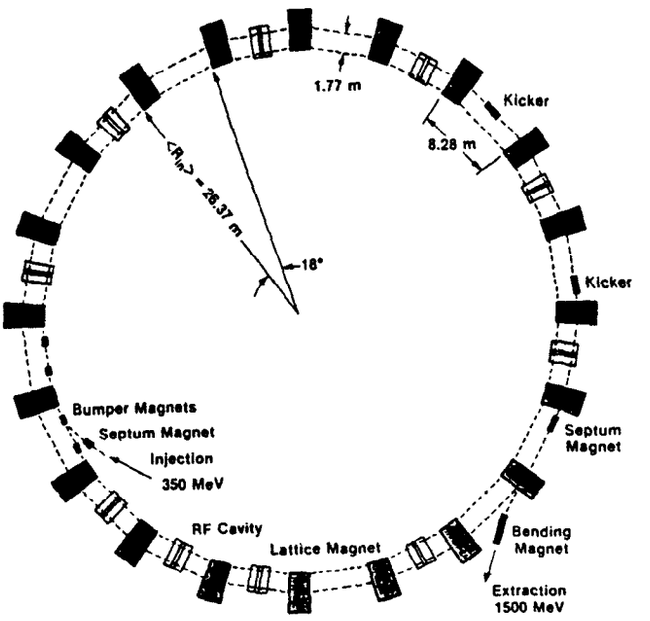

4. Schematic view of the 1500 MeV FFAG, radial type.

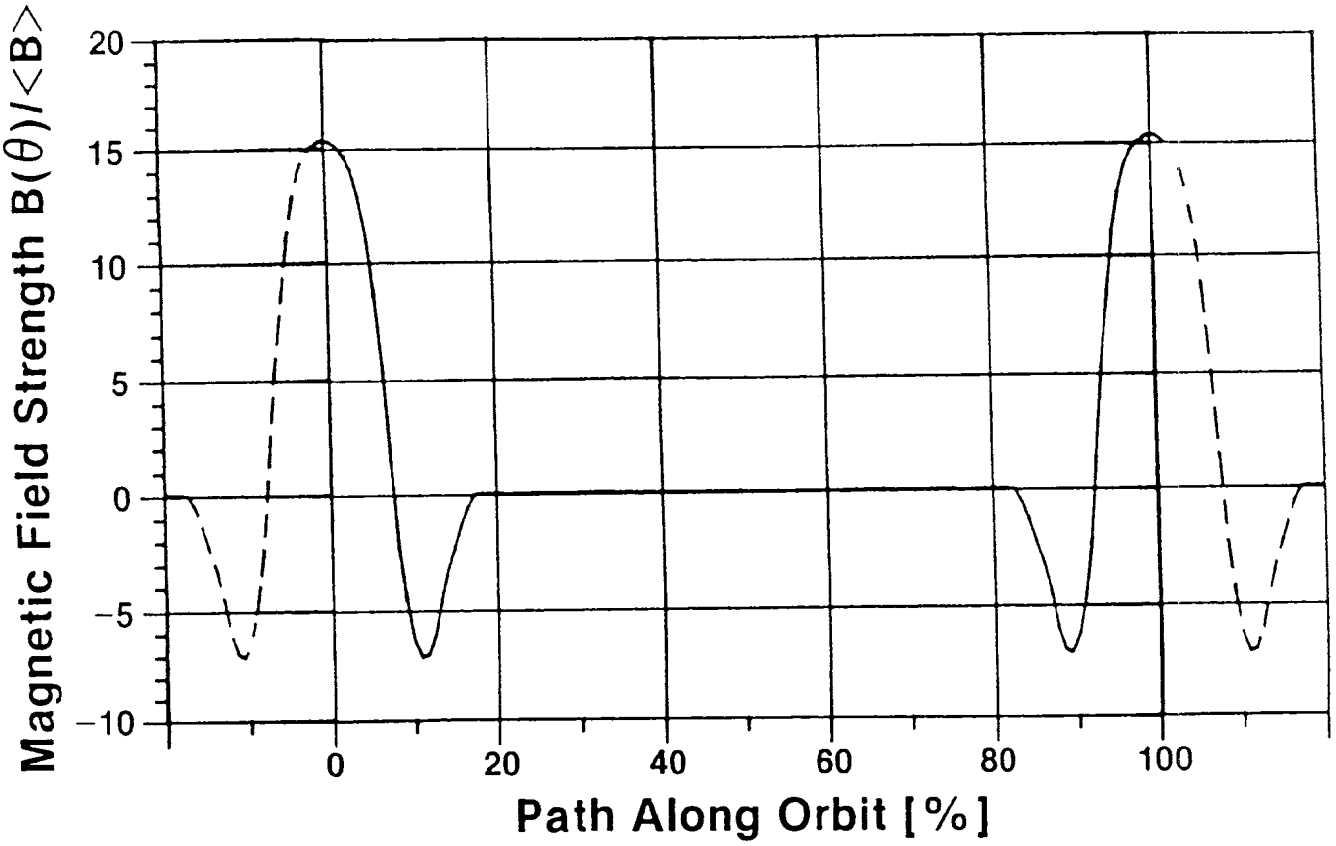

5. The azimuthal profile of the magnetic field along one lattice cell.

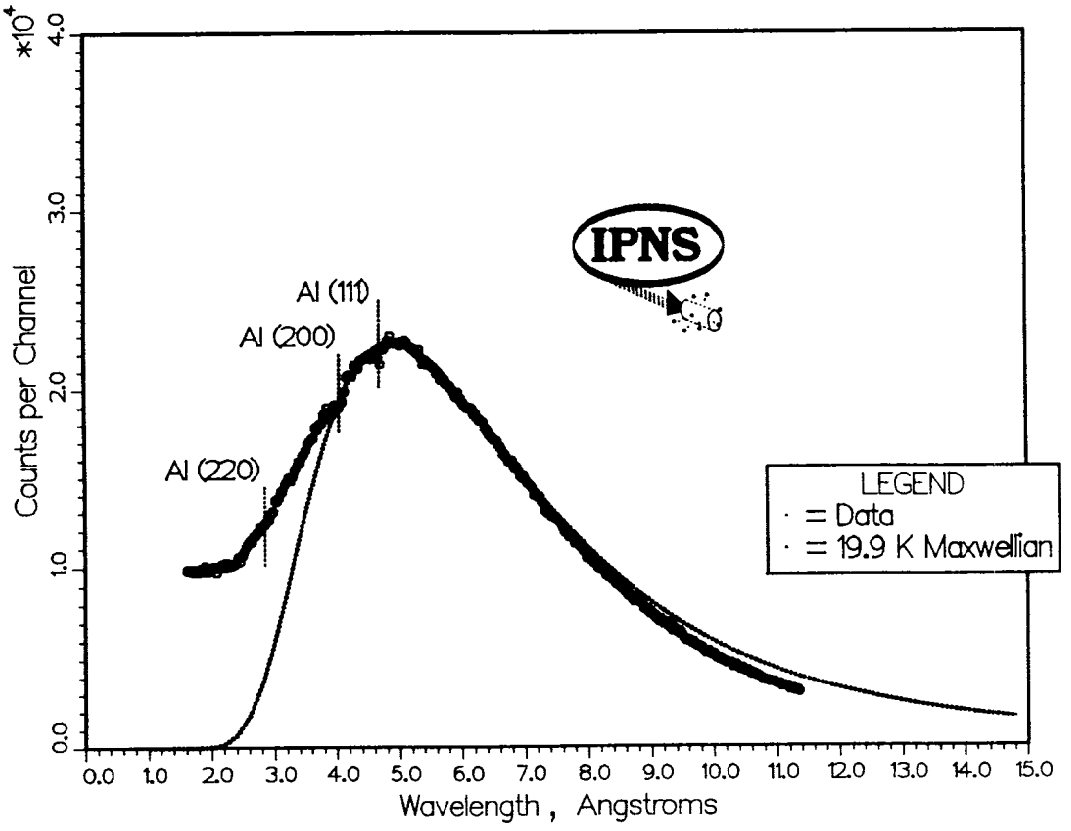

6. The counting rate distribution in a "1/v" detector from the 12 K solid methane moderator.

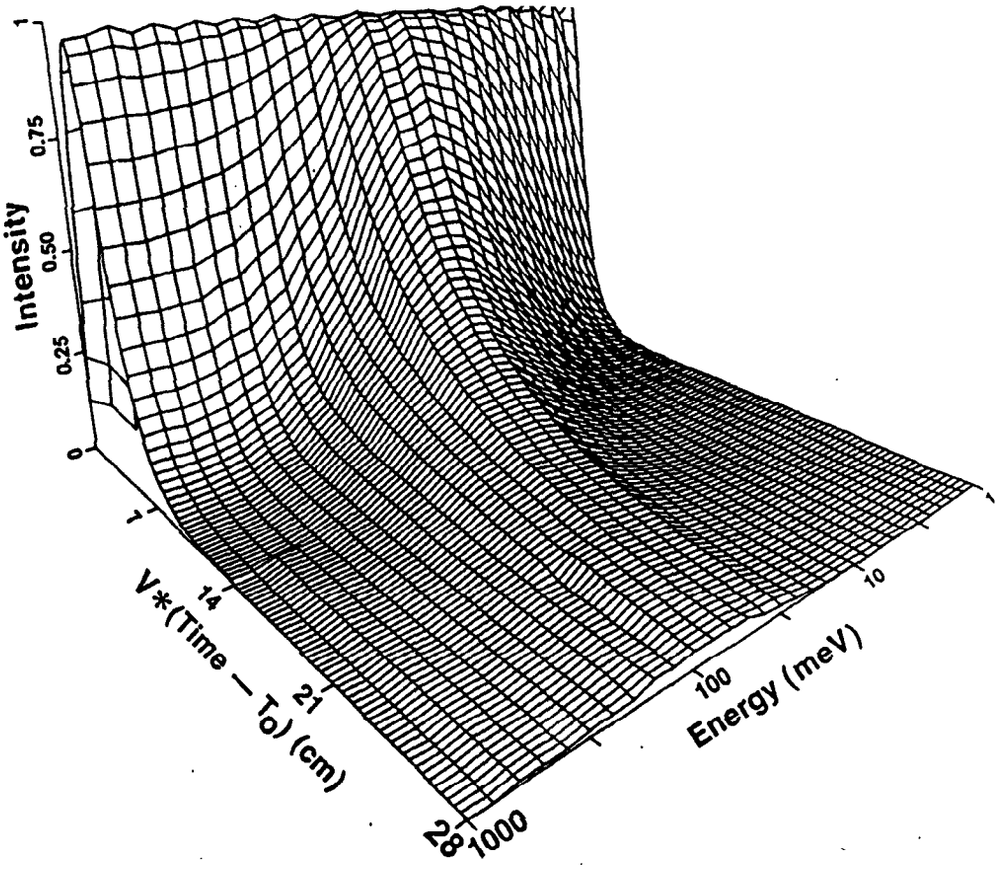

7. The pulse shape of the IPNS "H" moderator as a function of energy. Time is represented in length units $v*(t - t_o)$.

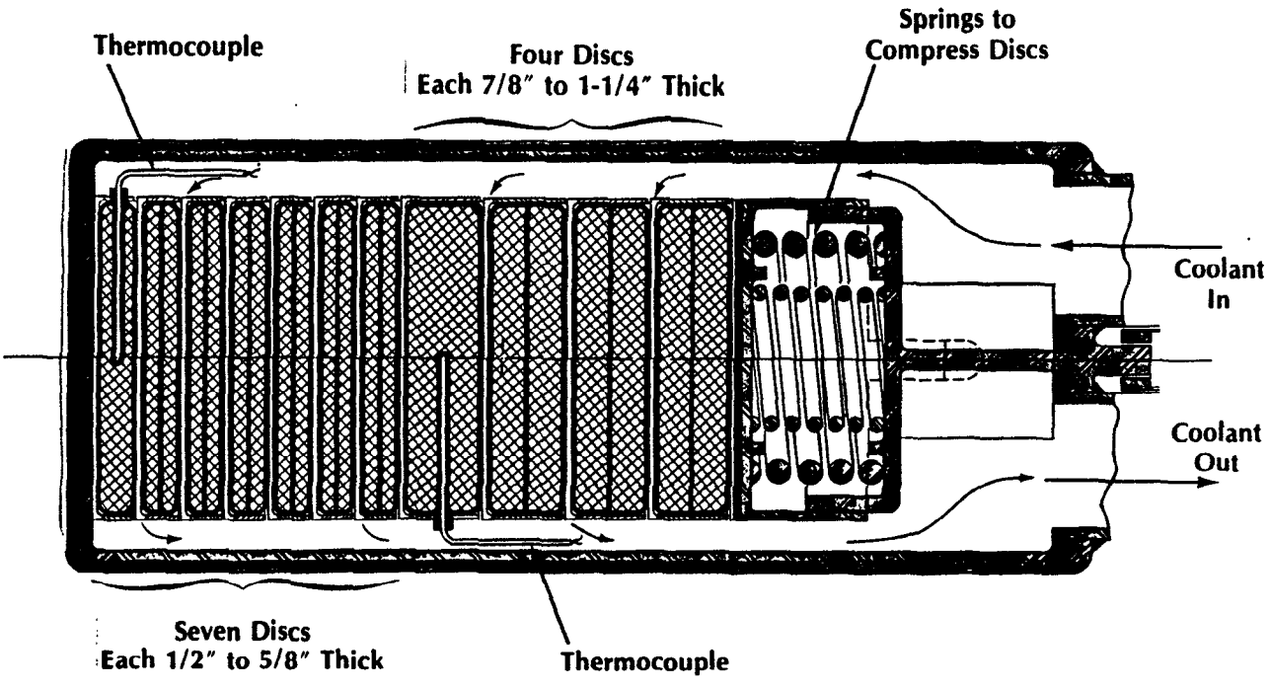

8. Cross sectional view of the Enriched Uranium Booster Target.

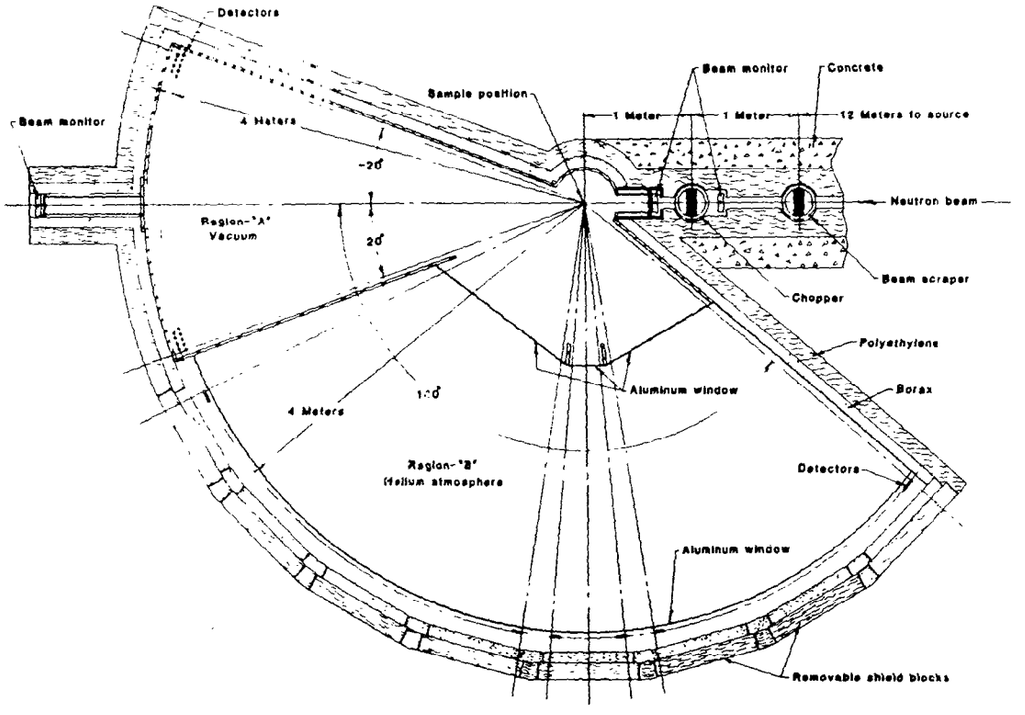

9. The High Resolution Medium Energy Chopper Spectrometer. The new flight path provides scattering angles between 90° and 140°.

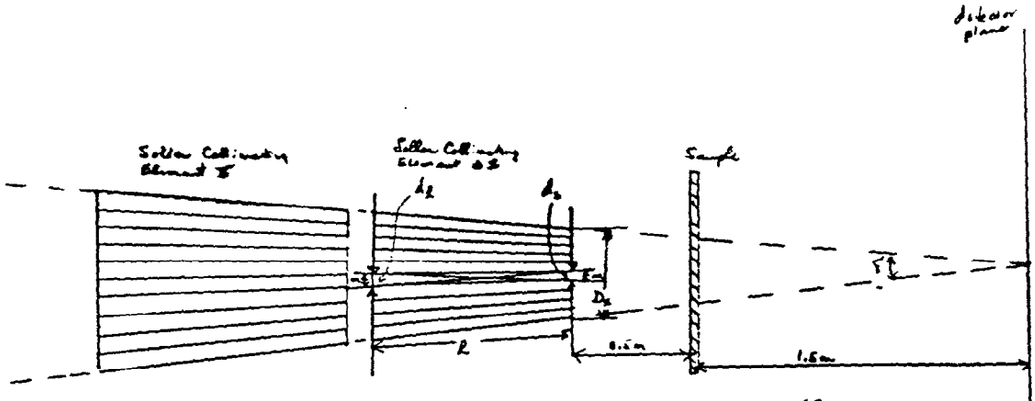

Focusing Soller Collimators, Aluminum coated with $^{10}_{5}B$

	d_s(mm)	d_ℓ(mm)	ℓ(cm)	D_s(cm)	δ(deg)	α(deg)
I).	0.750	0.844	25.0	1.63	0.4663	0.3653
II).	0.851	0.974	32.8	1.85	0.4663	0.3187

10. The multiple converging aperture collimator of the Small Angle Diffractometer.

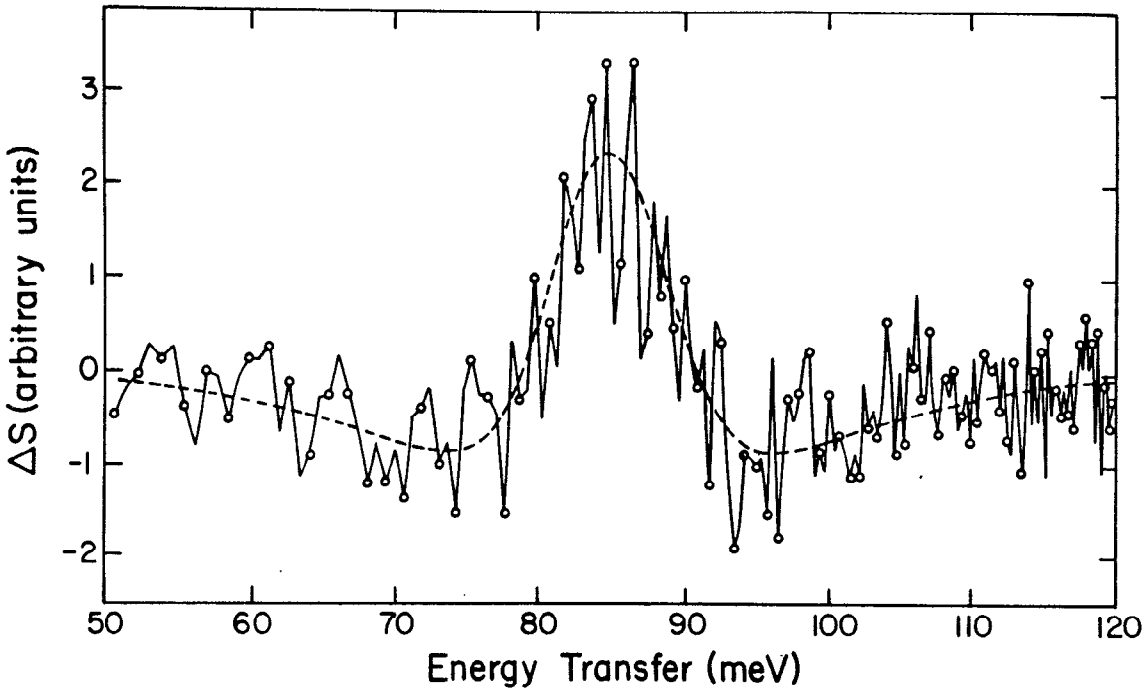

11. Difference between the inelastic scattering functions $S(Q,\varepsilon)$ of superfluid and normal liquid Helium, measured at the Low Resolution Medium Energy Chopper Spectrometer. The sharp peak is due to the Bose condensate.

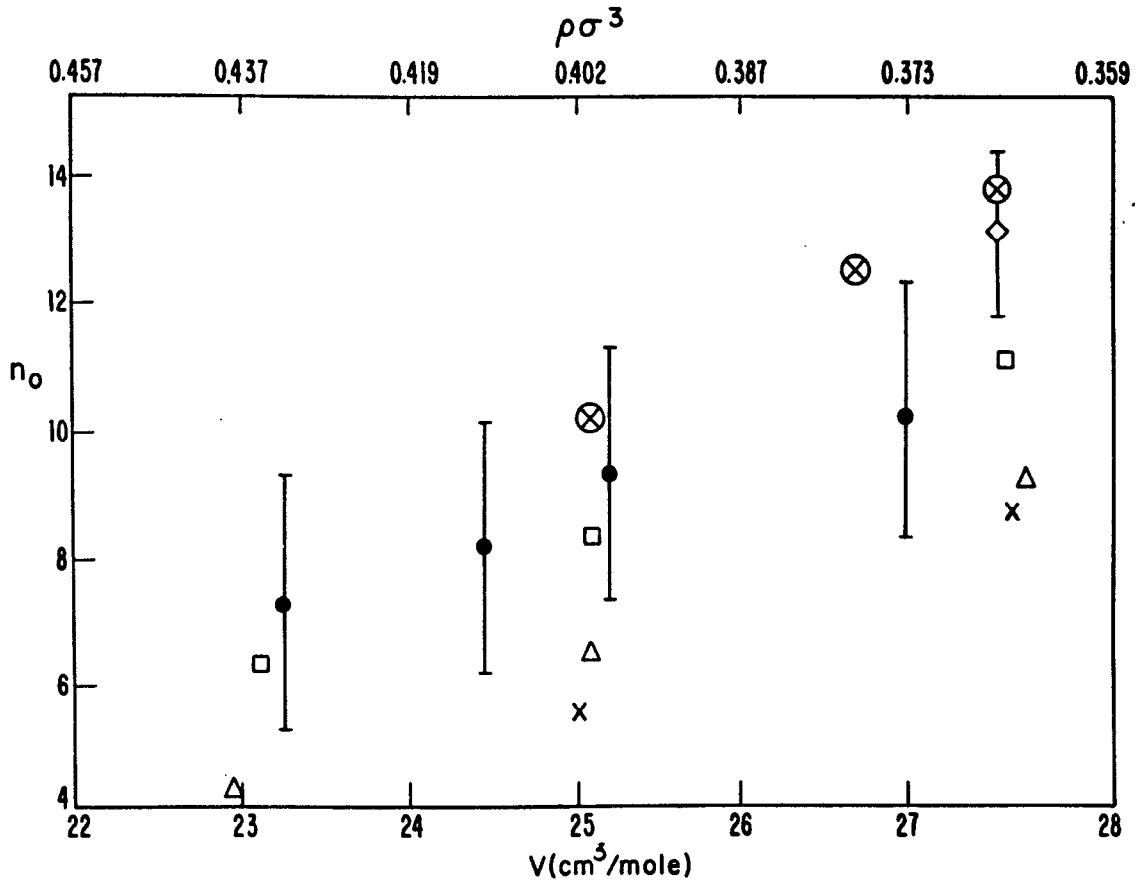

12. The Bose condensate fraction n_o of superfluid helium vs specific volume. Solid points with error bars are from LRMECS.

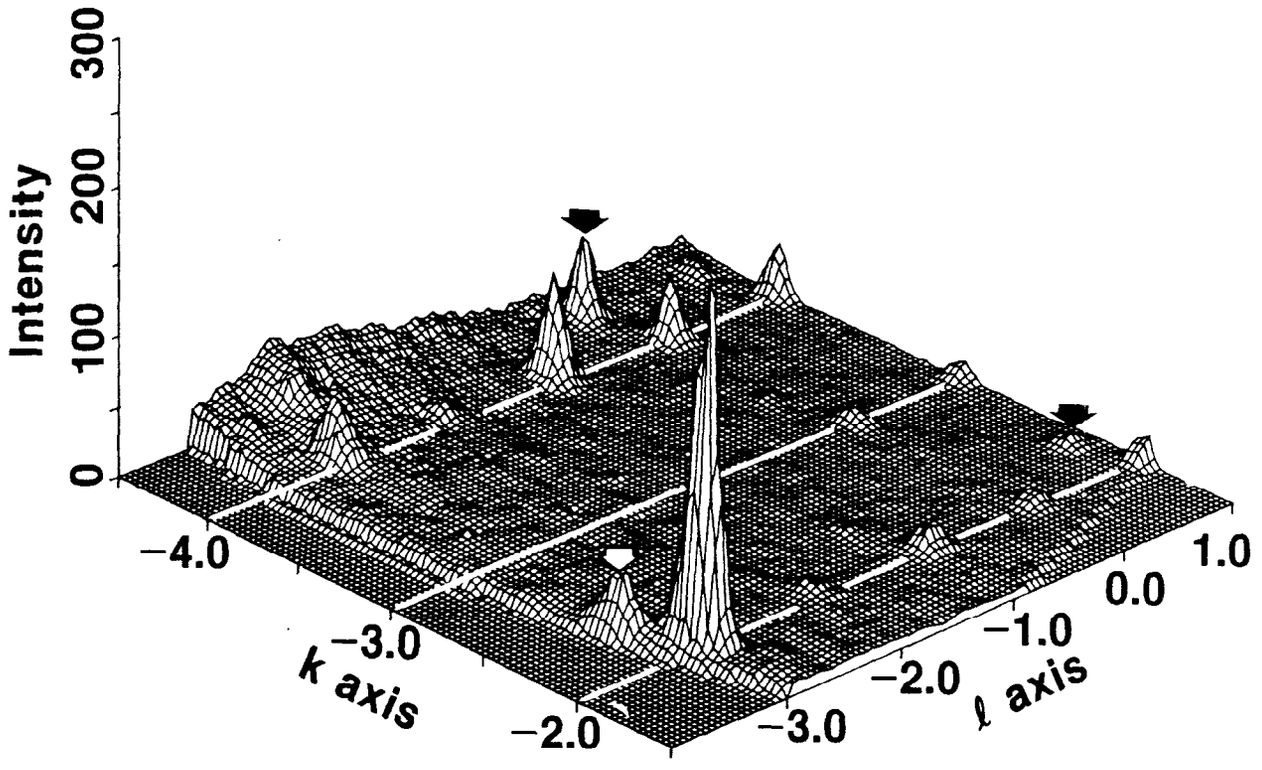

13. The diffracted intensity of $(BEDT\text{-}TTF)_2I_3$ at 20 K, in the (4.93,k,l) plane, measured on the Single Crystal Diffractometer. Arrows indicate superlattice peaks.

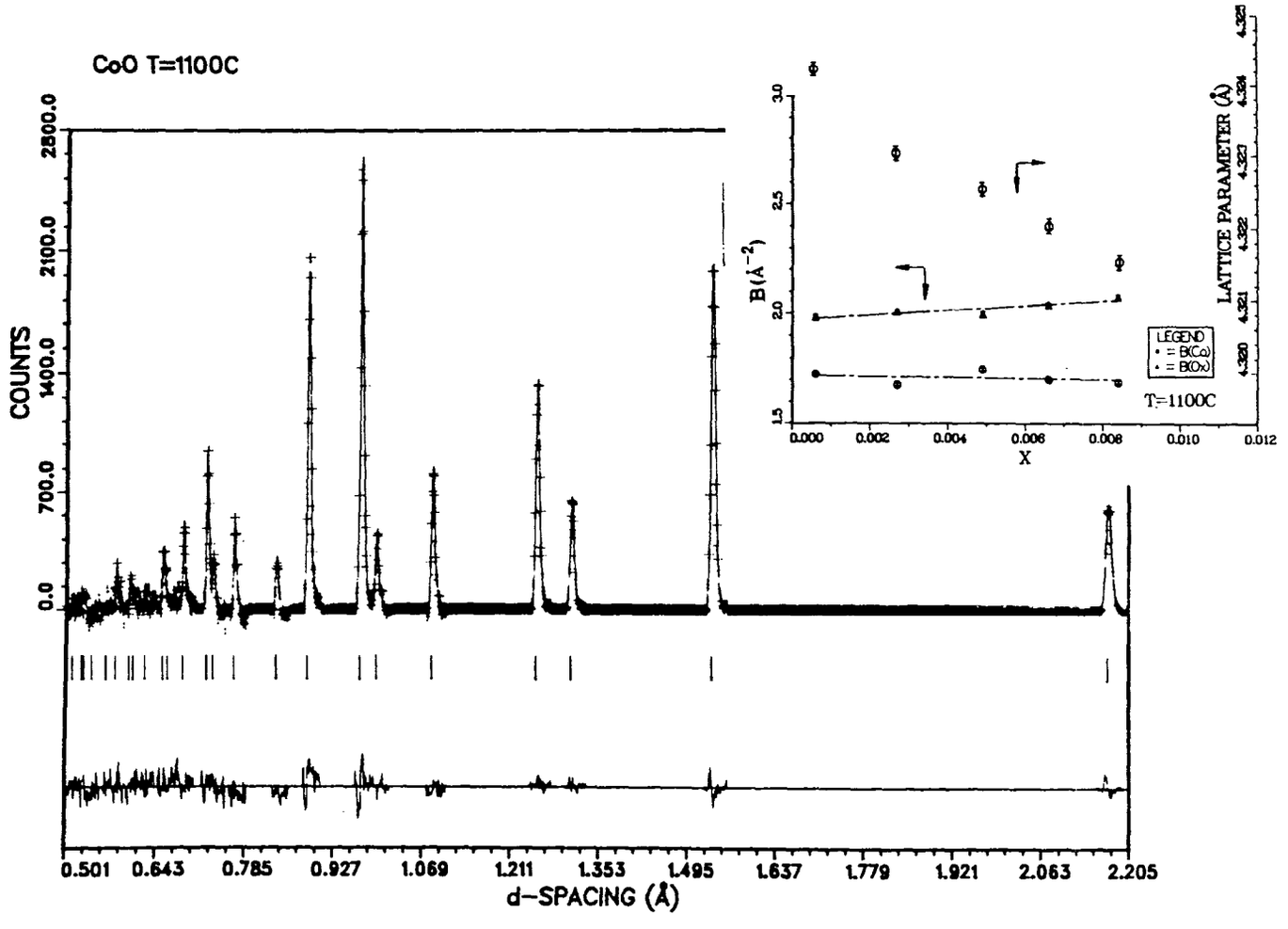

14. Powder diffraction pattern measured at $2\Theta = 90°$ on CoO(1-x)O at 1100 C in the General Purpose Powder Diffractometer. The inset shows the variation of lattice parameter and of the isotropic thermal parameters of Co and O.

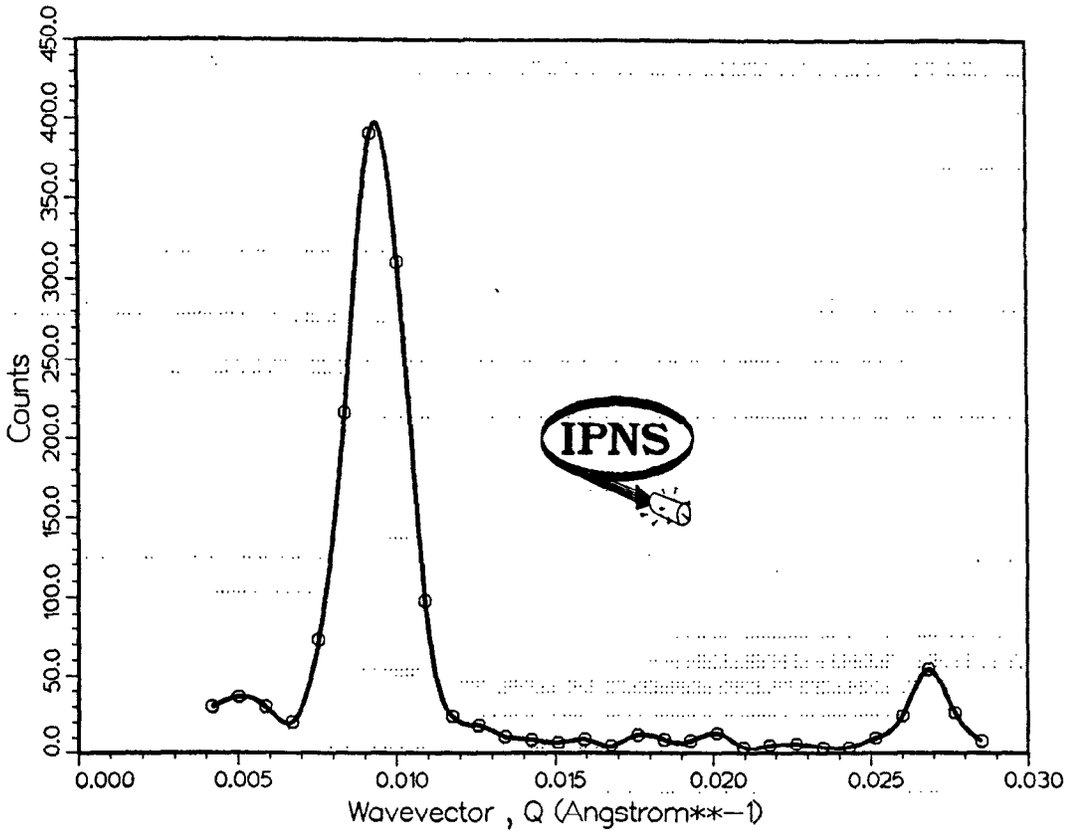

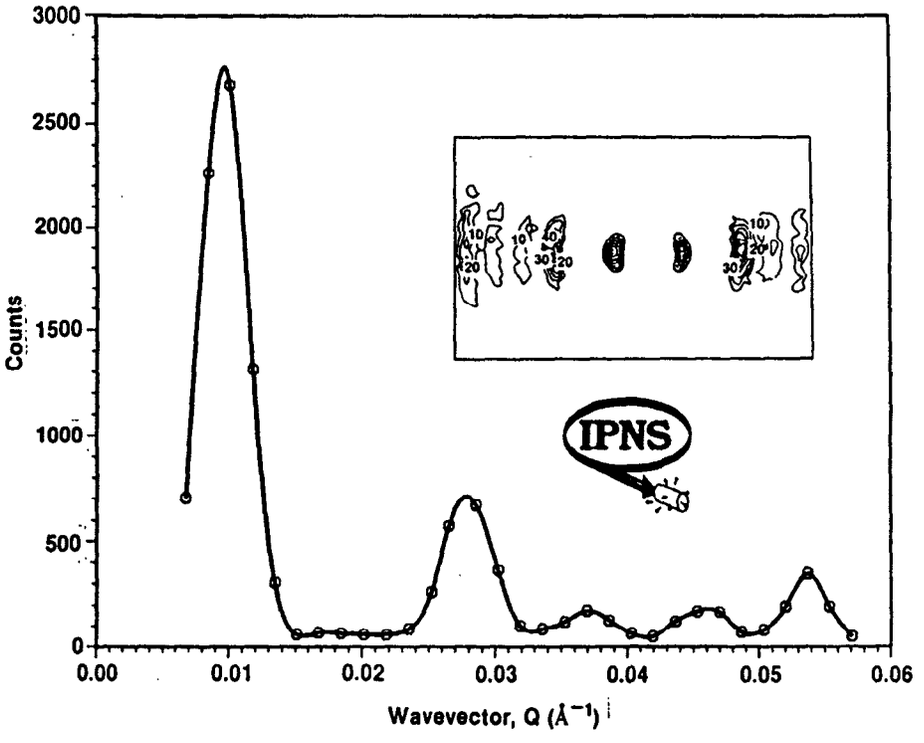

15. The Diffracted intensity from collagen of kangaroo tail tendon reconstituted in D_2O, measured on the Small Angle Diffractometer. a. From the 14. Å wavelength bin. b. From the 7. Å wavelength bin. The inset shows the intensity contours on the detector.

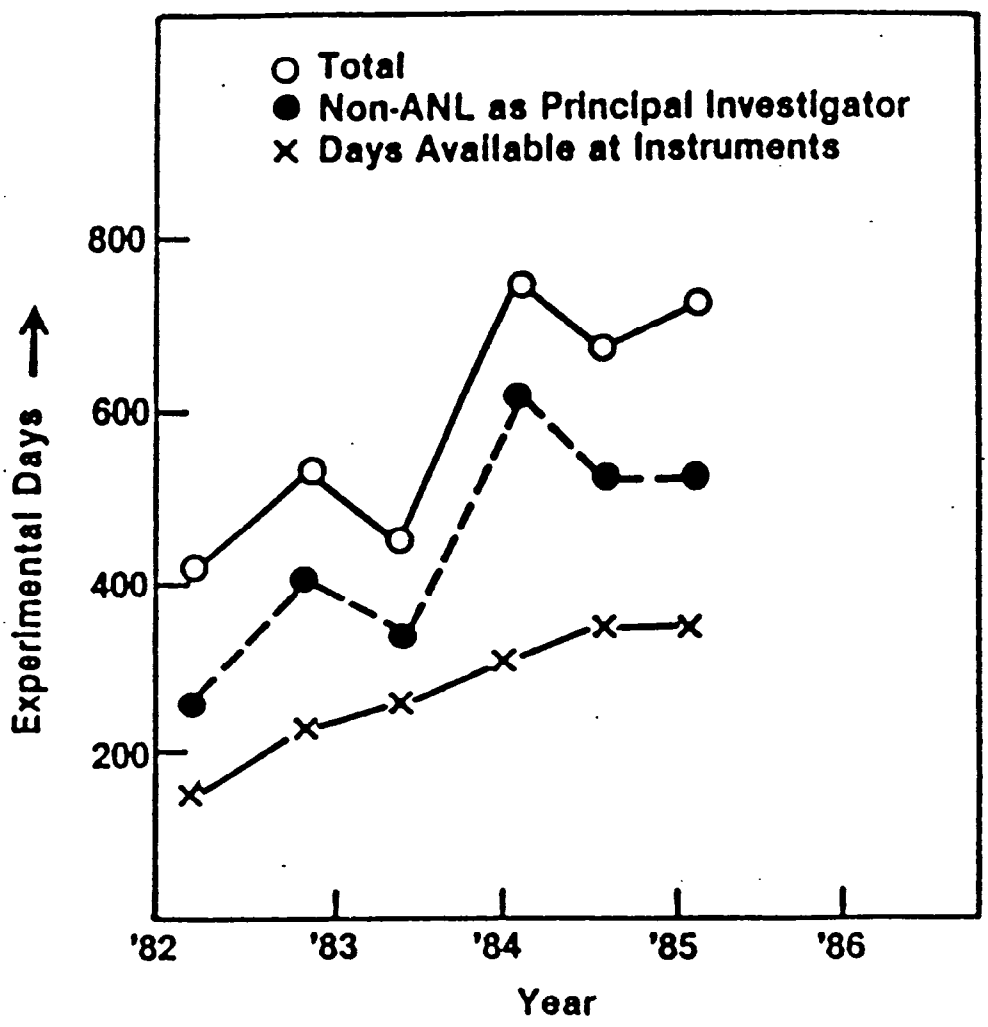

16. The number of experiment days requested and available for each six-month proposal period of IPNS.